Microstructural studies of aqueous sol derived ferroelectric $PbTiO_3$ thin films

2001 J. Phys.: Condens. Matter 13 501

(http://iopscience.iop.org/0953-8984/13/3/310)

INSTITUTE OF PHYSICS PUBLISHING JOURNAL OF PHYSICS: CONDENSED MATTER

J. Phys.: Condens. Matter **13** (2001) 501–513 www.iop.org/Journals/cm PII: S0953-8984(01)17343-1

Microstructural studies of aqueous sol derived ferroelectric $PbTiO_3$ thin films

R Bannerjee, S C Purandare, V R Palkar[1] and R Pinto

Department of Condensed Matter Physics and Materials Science, Tata Institute of Fundamental Research, Mumbai 400005, India

Received 21 September 2000, in final form 4 November 2000

Abstract

Aqueous sol derived ferroelectric $PbTiO_3$ thin films have been deposited on Si(100) substrates. Films crystallized by annealing at 675 °C, which exhibit the best ferroelectric properties and also excellent varistor-type behaviour, have been investigated in detail by TEM and x-ray diffraction. There is a partially preferred orientation of the crystallized grains of the perovskite phase along the (110) and (101) directions. During annealing, Si from the substrate diffuses into the films and forms an amorphous Si–O rich phase at the boundaries of the equiaxed grains of the perovskite phase. The formation of this amorphous phase is expected to increase the resistivity of the grain boundaries and consequently promote varistor-type behaviour. Domains were observed within the equiaxed grains and they exhibited a needle-like morphology. In a single grain, either a set of parallel domains or two sets of differently oriented parallel domains were observed. With increased diffusion of Si from the substrate, the fraction of the amorphous phase in the microstructure increased. The amorphous phase penetrated the domain boundaries within a single grain, eventually isolating the needle-like domains. The resulting microstructure consisted of needles of the perovskite phase in an amorphous matrix.

1. Introduction

Ferroelectric thin films are being widely researched for their potential application in future non-volatile memory devices such as non-volatile ferroelectric random access memories (NVFRAM). There is tremendous potential for developing novel field-effect devices by combining a ferroelectric material with a semiconductor. Such devices would exploit the basic electrical properties of the semiconductor appropriately modified by the polarization state of the ferroelectric [1]. The integration of ferroelectric thin films with existing silicon integrated circuit technology for the fabrication of microelectromechanical (MEMS) systems would be a focal point of future research activities [2]. In an earlier review of ferroelectric-semiconductor devices, it was reported that a device which uses a thin layer of ferroelectric

[1] Corresponding author.

0953-8984/01/030501+13$30.00

on a bulk semiconductor substrate is much more stable than a device which uses the reverse configuration with a thin semiconductor layer on a ferroelectric substrate [3].

Lead titanate ($PbTiO_3$) is a well known ferroelectric material which exhibits excellent dielectric, pyroelectric and piezoelectric properties. It belongs to the perovskite group of compounds and has the highest tetragonal distortion ($c/a \sim 1.063$) among the compounds of the perovskite group. Therefore, this compound is a good candidate for coupling with semiconductor Si substrates to fabricate ferroelectric-semiconductor devices. With this objective, $PbTiO_3$ thin films have been deposited on Si substrates with/without buffer layers using a variety of techniques including sputtering, pulsed laser deposition (PLD), sol–gel methods and chemical vapour deposition (CVD) [1]. Of all these techniques, sol–gel processing, which is a solution based technique, is economically the most attractive as it requires inexpensive equipment and raw materials. Furthermore, sol–gel processing also allows for the deposition of uniform thin films of large area. Carper and Phule [4] have discussed a novel spin-on process based on molecularly modified titanium precursor and hydrated lead acetate used to deposit ferroelectric thin films of $PbTiO_3$. Other studies on sol–gel processing include using lead acetylacetonate as the lead precursor, which decomposes and crystallizes into $PbTiO_3$ [5], and using lead acetate trihydrate and titanium isopropoxide in a solvent of 2-methoxy propanol [6]. Palkar *et al* [7] have developed a novel aqueous sol route for the deposition of $PbTiO_3$ thin films which simplifies the chemical processing and also avoids the use of dangerous chemicals. Thus, ferroelectric thin films of $PbTiO_3$ were directly prepared on Si(100) substrates for the first time by spin coating an aqueous sol containing lead and titanium hydroxy complexes and subsequently annealing at different temperatures. The authors reported that the ferroelectric properties of these sol processed films were comparable to those obtained by the complex alkoxide route and other expensive techniques [7].

Interestingly, in addition to good ferroelectric properties, the aqueous sol processed $PbTiO_3$ thin films deposited by Palkar *et al* exhibited good varistor properties. The current–voltage (I–V) characteristics of these films were found to be dependent on the processing parameters, specifically on the temperature of annealing. The films annealed at temperatures in the range of 600–700 °C exhibited high resistivity in the initial ohmic conduction region and a strong varistor type of behaviour while those annealed at higher or lower temperatures did not exhibit such good properties [8]. The results were interpreted qualitatively by the authors by considering the influence of grain boundaries on the conduction process in these films. However, the interpretation is based on speculations and there is no direct experimental evidence. It is well known that grain morphology, grain boundary structure, domain alignment etc play a very crucial role in determining material properties. Therefore, it is important to study the processing–microstructure–property relationships in these films especially if interaction between substrate and the film is likely to occur during processing. Transmission electron microscopy (TEM) is a very useful tool for probing the microstructure. In this paper, results of a detailed microstructural characterization of these films using TEM are discussed. Attempts are made to correlate the electrical conductivity to the observed microstructural features.

2. Experiment

The ferroelectric $PbTiO_3$ thin films have been prepared using an aqueous sol route. The details of the process are discussed elsewhere [7]. In the process, sol made up of ultrafine particles of the hydroxy complex in aqueous medium is deposited directly on Si(100) substrates by spin coating. Subsequent to deposition, the amorphous films have been furnace heated to convert the hydroxy complex into the perovskite $PbTiO_3$ phase. A variety of different crystallization temperatures, ranging from 500 to 850 °C, have been used. However, in the

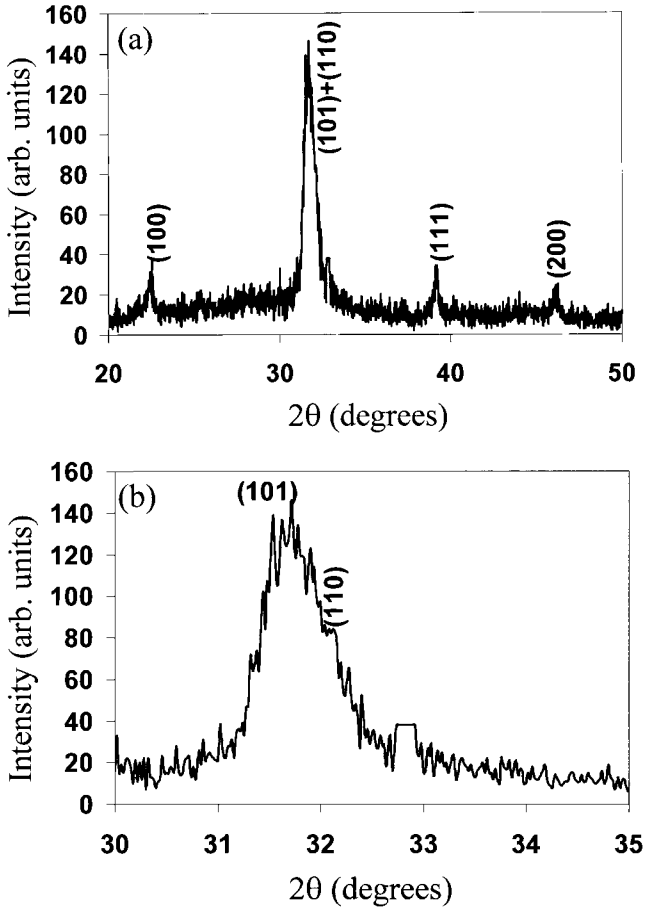

Figure 1. (a) X-ray diffraction pattern from the aqueous sol derived $PbTiO_3$ film. (b) A magnified view showing the should in the (101) peak arising due to the (110) peak.

present investigation, details of the microstructure and phase evolution in the films crystallized at 675 °C for four hours, exhibiting the most promising ferroelectric properties and varistor-like behaviour, will be discussed.

X-ray diffraction studies on the films were carried out by using Siemens D500 diffractometer operating at 25 kV and 35 mA. The incident radiation used was Cu Kα. For TEM, using a Gatan ultrasonic drill, 3 mm discs were drilled from pieces of the silicon wafer with the film deposited on it. As a precautionary measure to protect the thin film, the drilling was carried out from the substrate side. These discs were mechanically ground to a thickness of $\sim$120 μm on abrasive paper. Subsequently, the thinned discs were mechanically dimpled from the substrate side till the centre thickness was $\sim$20 μm. Dimpling was carried out using a Gatan dimple grinder. Finally, the dimpled specimens were ion milled in a Gatan Duo mill until there was a perforation at the centre. Argon ions of energy 6 kV, at an incident angle of 12°, were used during the ion-milling process. Electron transparent regions are formed near the edge of the perforation in the specimen. The TEM studies were carried out in a Philips CM200 TEM operating at an accelerating voltage of 200 kV. The TEM was equipped with an EDAX detector, which was used for elemental analysis.

Table 1. EDS analysis of the different regions in the film.

Region	Element	Composition (atomic %)
Equiaxed grains	Pb	22
	Ti	14
	Si	5
	O (balance)	59
Grain boundary	Pb + Ti	0.5
	Si	21
	O (balance)	78.5

3. Results

The x-ray diffraction spectrum from the $PbTiO_3$ thin film annealed at 675 °C is shown in figure 1(a). The peaks in this pattern can be indexed as the (100), (101) + (110), (111) and (200) diffracted intensities from the perovskite $PbTiO_3$ phase. The most intense peak lies at $2\theta \sim 32^\circ$. The asymmetry in this peak arises due to the overlap of the (101) and (011) peaks of the perovskite phase. Careful analysis of this peak reveals the presence of two intensity maxima in this peak, the first one at $2\theta \sim 31.4^\circ$ corresponding to (101) and the second one at $2\theta \sim 32.4^\circ$ corresponding to (011). This also leads to an asymmetry in the peak as evident from figure 1(b). Based on the interplanar spacings of these and other peaks in the pattern, the lattice parameters of the perovskite phase in this film have been calculated as $a = 0.394$ nm and $c = 0.407$ nm. These lattice parameter values are comparable to those reported by other workers [9, 10]. Another interesting feature of the x-ray pattern is that the (100) and (111) peaks are of a very low intensity. In a randomly oriented polycrystalline film, the relative intensities of the (100), (101), (110) and (111) peaks are expected to be 50, 100, 55 and 40% respectively [11]. However, in the pattern shown in figure 1, the relative intensities of these four peaks are 18, 100, 56 and 18% respectively. Therefore, it appears that there is a preferential texturing of the grains along the (101) (or (011)) direction in this film. This is further corroborated by the x-ray diffraction results from aqueous sol derived $PbTiO_3$ films crystallized at temperatures of 600 and 700 °C, presented in an earlier paper [7], wherein the perferential (101) + (110) texture is also observed.

A low magnification TEM micrograph from the film crystallized at 675 °C, shown in figure 2(a) reveals cracks in certain regions of the films (the regions of light contrast in the micrograph). It is important to note that, though the film is cracked in certain areas, there is interconnectivity between the various regions of the film. The cracks have not propagated to the extent of electrically insulating different areas of the film. Energy dispersive spectroscopy (EDS) was carried out in order to ascertain the identity of these cracks in the film. The analysis revealed the primary presence of Si and a small amount of oxygen in these regions, confirming that these regions correspond to the Si substrate. The overall microstructure of the film is shown in a higher magnification bright field micrograph (figure 2(b)). The grains of the perovskite $PbTiO_3$ phase appear to be separated by a thin layer of a different phase at the grain boundaries, which exhibits a lighter contrast in the micrograph. Most of the perovskite grains have an equiaxed morphology, which is apparent from figure 2(b). In addition to the equiaxed grains, there appear to be a smaller fraction of grains of an acicular morphology (needle-like) present in certain regions of the film (figure 2(c)). The average size of the equiaxed grains is ∼300–400 nm whereas the needle-like grains are of the size of 300 nm × 30 nm (the aspect ratio is ∼10:1). A representative EDS spectrum from one of the equiaxed grains is shown in figure 3(a) while a sample spectrum of the grain boundary phase is shown in figure 3(b).

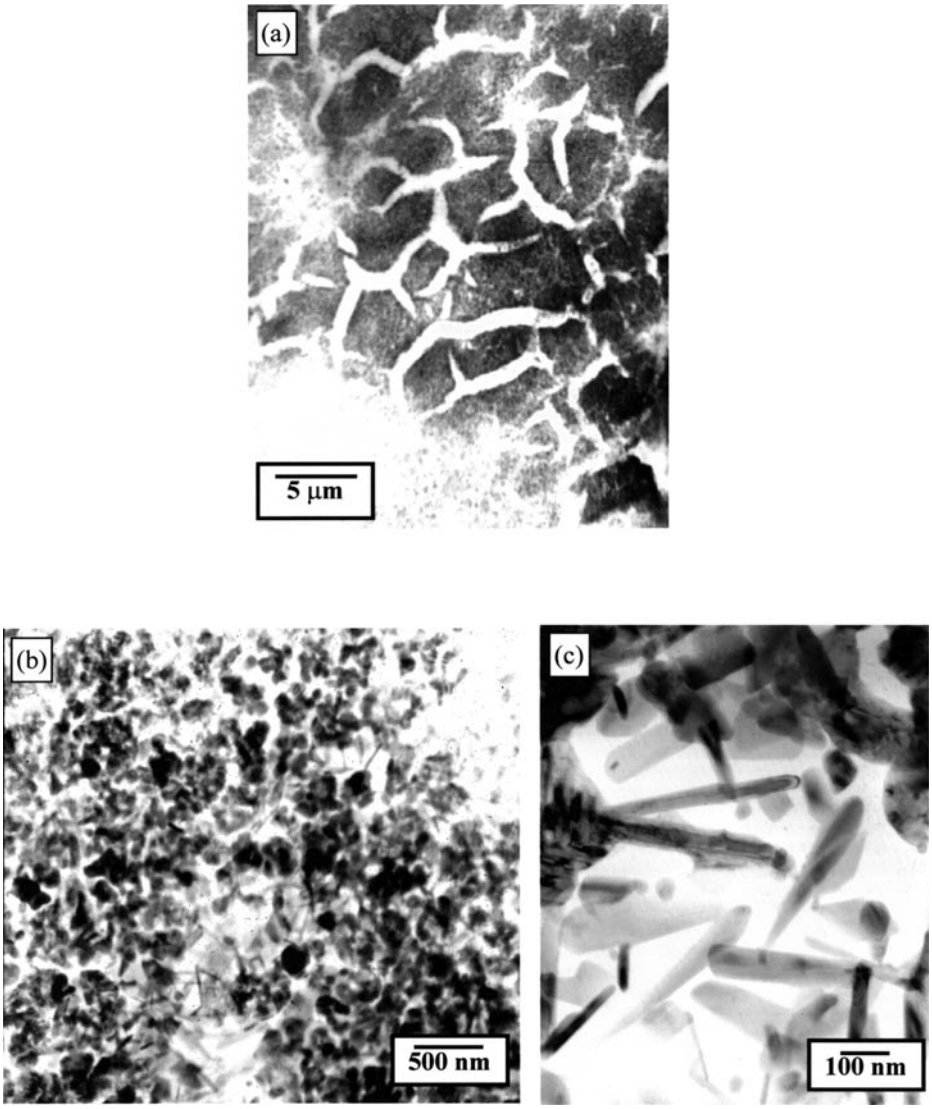

Figure 2. (a) A low magnification TEM micrograph showing cracks in the aqueous sol derived $PbTiO_3$ film. (b) A bright field TEM micrograph showing the overall microstructure of the film. (c) Grains of the perovskite are bounded by a layer of the amorphous phase at the grain boundary.

The approximate formula arrived at from the EDS elemental analysis (table 1) for the equiaxed grains is $Pb(Ti_{0.75}Si_{0.25})O_3$.

A large aperture selected area diffraction (SAD) pattern from the thin film is shown in figure 4(a). The diffracted rings can be indexed based on the perovskite structure. Care was taken to avoid diffraction intensities from the Si substrate by selecting an appropriately thin region of the specimen. An important feature to note in the SAD pattern shown in figure 4(a) is the non-uniform intensity distribution of the rings with the most intense diffracted ring corresponding to the (100) + (001) planes of the perovskite phase. This is supportive of the presence of a partial texture in this thin film. Furthermore, single crystal SAD patterns recorded

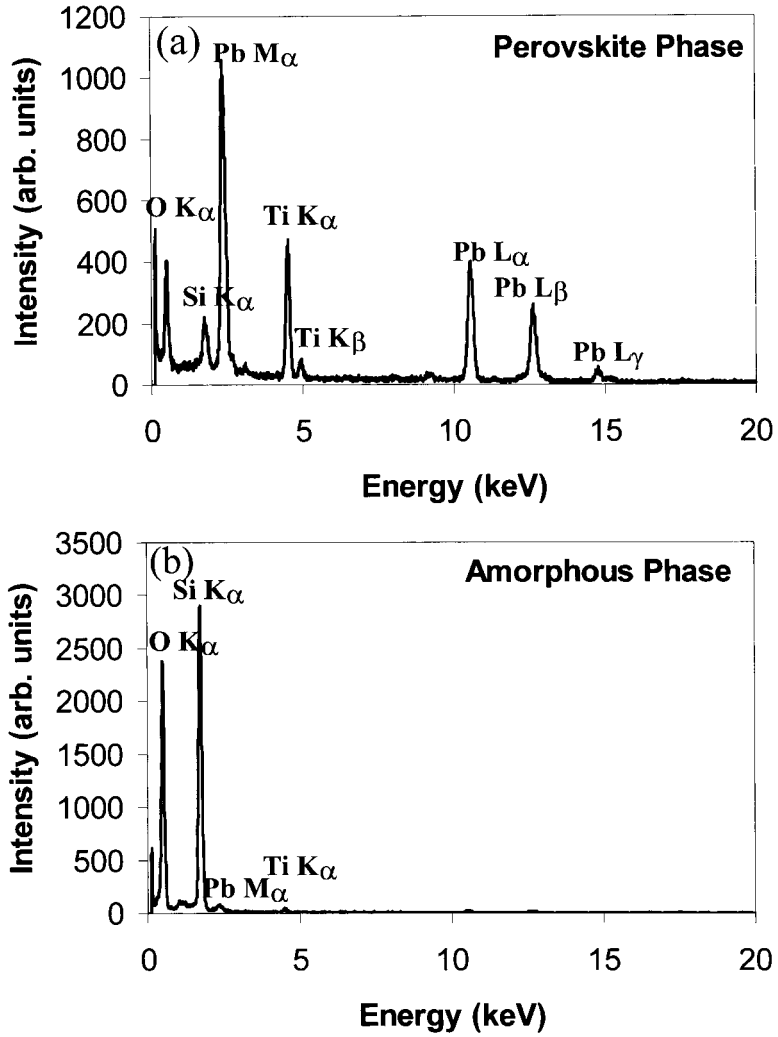

Figure 3. EDS spectra from the perovskite phase (a) and the amorphous phase (b).

from a number of grains revealed that their normals were aligned close to the (101) or (110) directions. Representative (101) and [133] zone axis SAD patterns are shown in figure 4(b) and figure 4(c) respectively. In order to determine the structure of the Si–O rich phase of lighter contrast, a small aperture SAD pattern was recorded (figure 4(d)). It is apparent from this pattern that the phase is amorphous or glassy in nature. As stated earlier, this amorphous phase is present along the grain boundaries of the perovskite phase. In regions with higher density of needle-like grains, the microstructure can be described as grains of the perovskite phase embedded in an amorphous Si–O rich matrix (refer to figure 2(c)).

In the relatively thin regions of the TEM specimen, ferroelectric domains could be imaged within the equiaxed grains of the perovskite phase (figure 5(a)). Within the same grain, in many cases the sets of domains were oriented along different crystallographic directions. A higher magnification micrograph shown in figure 5(b) reveals a single grain consisting of two sets of domains oriented at an angle close to 110°, while within the same set, the domains are

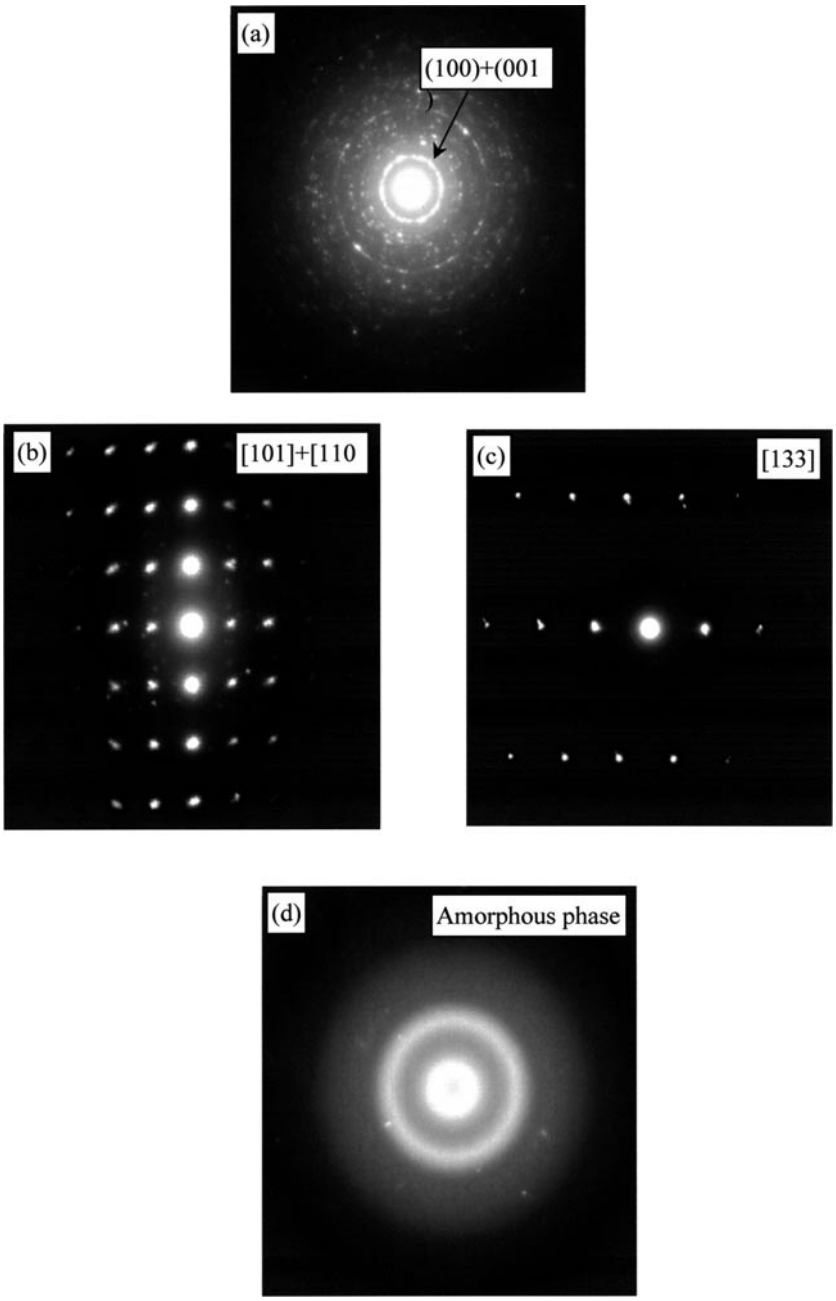

Figure 4. (a) A large aperture selected area ring diffraction pattern from the $PbTiO_3$ thin film. (b) A selected area diffraction pattern from a collection of the domains of $PbTiO_3$ exhibiting superposition of (101) and (110) zone axes. Note the arcing of the (111) spots in the pattern. (c) A (133) zone axis selected area diffraction pattern from a single $PbTiO_3$ domain. (d) A selected area diffraction pattern from the amorphous phase.

aligned parallel to each other. It should be noted that the SAD pattern from the whole grain can be indexed as the overlap of the (101) and (110) zone axes of the perovskite phase (refer

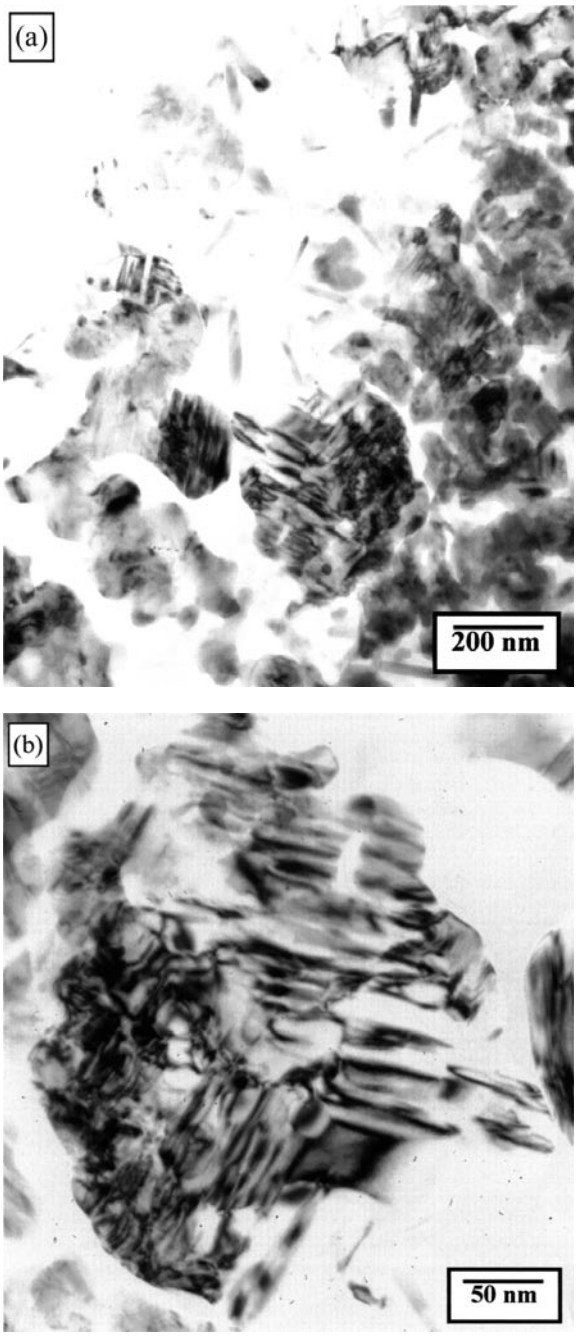

Figure 5. (a) A bright field TEM image showing domains within the grains of the perovskite $PbTiO_3$ phase. (b) A higher magnification TEM image showing two sets of domains misoriented by $\sim 110^\circ$ within a perovskite grain. (c) A schematic representation of the superposition of (101) and (110) zone axis diffraction patterns arising from different sets of domains within the same perovskite grain as shown in (b). The actual diffraction pattern is shown in figure 4(b). (d) A schematic diagram showing the arrangement of domains in the grain shown in (b) together with the crystallographic orientation relationships between the different sets of domains. The ferroelectric polarization axis (001) is also marked for each domain.

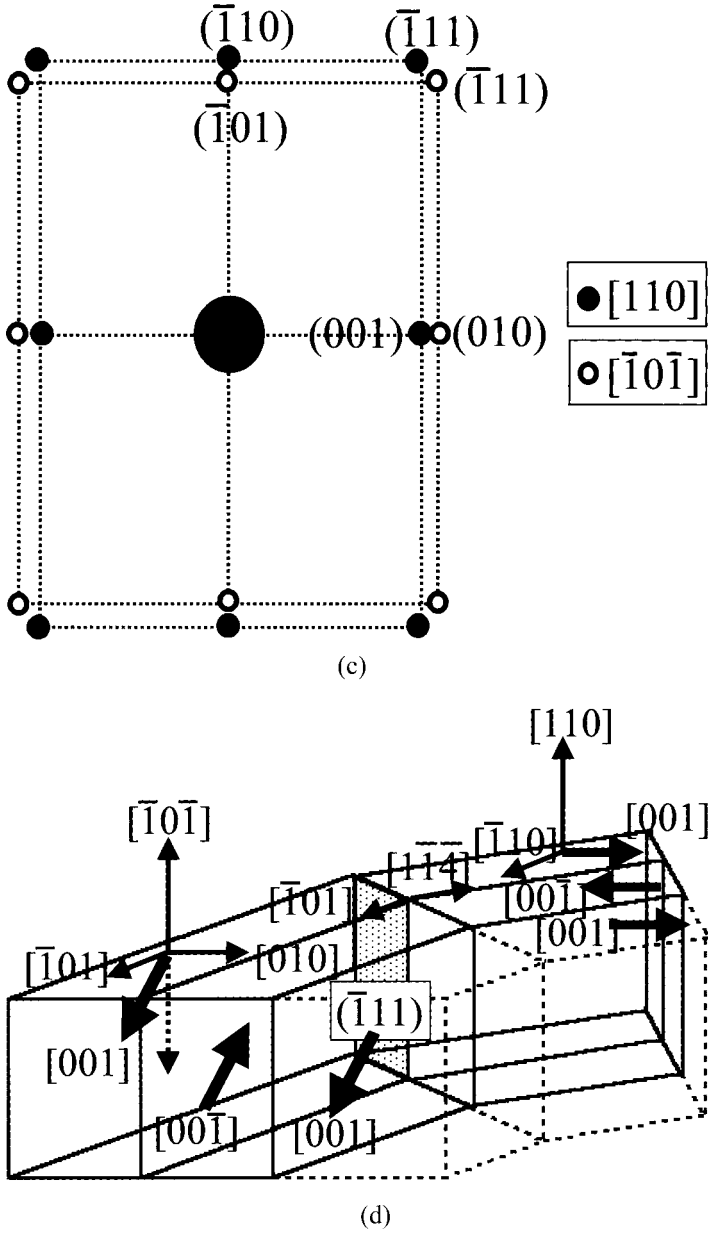

Figure 5. (Continued)

to figure 4(b)). The tetragonality in the perovskite phase implies a small mismatch between the (101) and (110) zone axis diffraction patterns. This has been schematically illustrated in figure 5(c). Since the lattice parameter is larger along the (001) axis, the (001) and ($\bar{1}$01) vectors in reciprocal space would be smaller than the (010) and ($\bar{1}$10) vectors. However, the length of all (111) vectors remains the same. Consequently, the overlap of the two zone axes results in an overlap of (111) spots which are radially misaligned and form small arcs in the diffraction pattern. Close inspection of the SAD pattern shown in figure 4(b) reveals such an

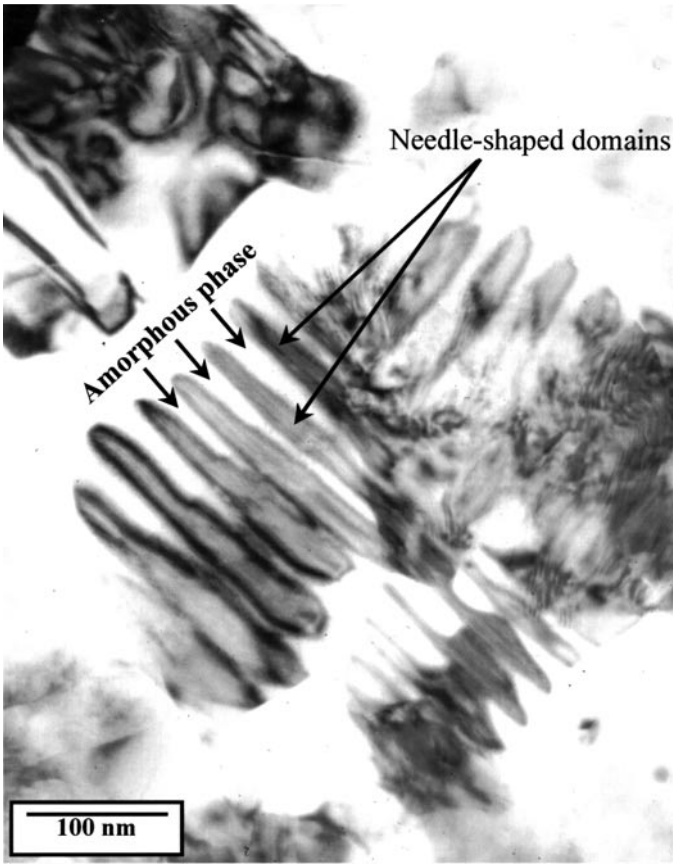

Figure 6. A TEM image exhibiting the increase in the volume fraction of the amorphous phase by penetrating into the domain boundaries within a grain of the perovskite phase. In the process, the amorphous phase isolated individual needle-like domains.

arcing of the (111) spots. The polarization vector in the $PbTiO_3$ phase is aligned along the (001) direction (*c*-axis). Therefore, based on the crystallographic analysis, the domains can be schematically described as shown in figure 5(d).

An interesting observation regarding the formation of domains is that all the needle-like grains appear to be single domain and do not exhibit any multi-domain contrast within individual grains. Furthermore, the aspect ratio and dimensions of these needle-like grains are similar to those of the individual domains within the equiaxed grains. A magnified view of an equiaxed grain containing a number of needle-like domains is shown in figure 6. Interestingly, it appears that the domains are separated by a layer of the amorphous Si–O rich phase. In effect, the amorphous phase appears to be penetrating at the domain boundaries and separating the individual domains into needle-like grains. As seen in figure 6, this process affects domains along the different orientations. Such a situation would warrant enrichment of the domain boundaries in the equiaxed grains with Si due to the diffusion process. The presence of the Si substrate in direct contact with the film implies an inexhaustible source of Si, which can increase the fraction of the amorphous phase in the film.

4. Discussion

Based on the compositional analysis of the equiaxed grains of the perovskite phase, it appears that the stoichiometry of the phase is close to $Pb(Ti_{1-x}Si_x)O_3$. It seems that though the ratio of PbO is maintained in the film, the ratio of Ti:O is lower than that for stoichiometric $PbTiO_3$. Some amount of Ti (∼5 at.%) appears to have been displaced from the perovskite phase by Si which has entered the film from the substrate. Though it is not possible to unequivocally establish that the Si atoms occupy the Ti sublattice in the perovskite phase, the composition suggests such a possibility. The observed reduction in TiO_2 content of the film is unexpected. In fact there are more chances of reduction in PbO content since it is a volatile component. The findings are certainly new and remarkable if the observed results are to be believed. The earlier report on Rietveld analysis of neutron diffraction data collected on an Si added $PbTiO_3$ bulk sample has indicated that Si does not occupy either the Pb or Ti site in the perovskite lattice of $PbTiO_3$ [12]. However, cautionary interpretation of the EDS results is required since there could be compositional changes introduced in the specimen during the process of ion milling. Pb, being a relatively heavy element, is expected to mill at a slower rate than Ti and consequently result in an artificial enrichment of Pb in thin regions of the TEM specimen.

A post-mortem analysis of the microstructural details of the aqueous sol derived $PbTiO_3$ thin film suggests a possible path for the development of different phases. This understanding is important since it has direct ramifications on the ferroelectric and varistor properties of these films. After spin coating the film containing the hydroxy complex is amorphous in nature and is in direct contact with the Si(100) substrate [7]. Decomposition of the hydroxy complex and consequent crystallization of the film is carried out by annealing it in a furnace at elevated temperatures. In the present study, the film was annealed at 675 °C for four hours. Grains of the perovskite phase form as a result of decomposition. These grains exhibit an equiaxed morphology and contain multiple domains. However, the elevated temperature allows diffusion of Si from the substrate into the film. The Si diffused in the film is perhaps causing two different effects. Part of it displaces ∼5 at.% Ti from the $PbTiO_3$ phase. A certain amount of Si reacts with PbO and forms a lead silicate-like glassy phase or reacts with $PbTiO_3$ to form an amorphous pyrochlore phase and segregates at the grain boundaries of the perovskite phase. The Si–O rich amorphous phase at the grain boundaries is likely to be comprised of a mixture of the lead silicate-like glassy phase and a small fraction of the pyrochlore phase. Based on the experimental observations, a possible mechanism can be proposed for the transformation in the grain morphology. The Si diffuses from the substrate into the amorphous Si–O rich phase at the grain boundaries of the equiaxed grains. Subsequently, the additional Si creates more amorphous phase by diffusing into the domain boundaries within the equiaxed grains. As a result, the needle shaped individual domains are separated by a layer of the amorphous phase, eventually leading to isolation of the grains in the amorphous matrix. The resulting microstructure is two phase. Such a situation corresponds to significantly large amounts of Si diffusion, which is reflected in a few regions of the film annealed at 675 °C (refer to figure 2(c)). By mass balance, it is likely that, with reducing volume fraction of the perovskite phase, the concentration of Pb and Ti increases in the amorphous phase.

The microstructural development in these films plays a pivotal role in determining the ferroelectric properties of these films. Palkar *et al* [7] have measures the saturation polarization (P_s), remnant polarization (P_r) and loss factor ($\tan\delta$) for films crystallized at various temperatures and concluded that the most promising properties for applications such as non-volatile memories are exhibited by films annealed in the range of 600–700 °C. Films annealed in this range of temperatures exhibited the largest value of P_s (35 μC cm^{-2}) and ratio of P_r/P_s (0.56), and the minimum value of $\tan\delta$ (0.02). Previously, scanning electron

microscopy (SEM) studies were conducted on films annealed at 500 and 800 °C for four hours each. In the case of the 500 °C sample, the microstructure consisted of small (∼50 nm) grains which were still in the process of development and therefore did not exhibit well defined grain boundaries. Nevertheless, the film exhibited reasonable ferroelectric properties, which was explained on the basis of short-range ordering and the presence of randomly oriented frozen dipoles [7]. The field needed to align these dipoles is quite large and reduces as the crystallinity in the film develops with higher annealing temperatures. Films annealed at 675 °C for four hours, which have been investigated in the present study, exhibit well-defined grains and boundaries. The boundaries are wetted by an Si–O rich amorphous phase resulting from the diffusion of Si from the substrate into the film. Though the amorphous phase at the boundaries is expected to be non-ferroelectric, most of the film consists of large (∼300–400 nm) well-defined grains of the perovskite phase and consequently exhibits good ferroelectric behaviour and low loss factor. The insulating nature of the grain boundaries helps in keeping the loss factor low. Extended exposure to the same temperature or annealing at higher temperatures results in additional diffusion of Si from the substrate and a consequent increase in the fraction of non-ferroelectric amorphous phase. The microstructure consists of a two-phase mixture of needles in the perovskite phase in an amorphous matrix, which is seen in some regions of the film annealed at 675 °C (refer to figure 2(c)) as well as in the SEM studies of the film annealed at 800 °C [7]. This contributes to an increase in the loss factor (0.087) as well as a reduction in the value of P_s (14 μC cm^{-2}) [7].

In addition to ferroelectric properties, excellent varistor-type behaviour is also exhibited by the $PbTiO_3$ films crystallized at temperatures in the range of 600–700 °C. The varistor-type properties of these films have been attributed to grain boundary limited conduction (GBLC). The GBLC model is based on the idea that the well developed grain boundaries in a material can act as resistive barriers to conduction by trapping charge carriers. Since the grain boundary is significantly more structurally disordered and chemically inhomogeneous than the grain interior, highly localized electronic states are created in the forbidden gap [13]. By interacting with the charged carriers responsible for conduction in the material, the grain boundary states can trap these carriers and consequently the boundaries become charged. If the trapped species are the charge carriers, potential barriers are created at the grain boundaries that make them highly resistive to current flow [14, 15]. During post-deposition annealing of the $PbTiO_3$ films, due to lead losses a certain number of Pb vacancies are created, which tend to segregate towards the grain boundaries since these are energetically favourable sites for the residence of such vacancies [14]. The segregation of these vacancies leads to the grain boundaries becoming charged and creates a depletion layer and a potential barrier at the boundaries. Furthermore, due to the finer grain sizes in these films, the depletion regions of two adjacent grains can overlap and a double depletion layer is formed, which can account for their strong varistor-type characteristics [8, 13]. From the results of the current study it is possible to conclude that, in addition to charge trapping, the presence of a second phase at the grain boundaries can also increase their resistivity. In the case of the crystallized sol derived $PbTiO_3$ thin films on Si it appears that the amorphous Si–O rich layer at the grain boundaries contributes to their enhanced resistivity. The amorphous phase also acts as an excellent trapping site for the vacancies since it is energetically highly favourable for the vacancies to reside in the amorphous phase rather than in the bulk of the crystalline perovskite grain.

5. Conclusion

Ferroelectric films of $PbTiO_3$ have been deposited on Si substrates by an aqueous sol based spin coating process; these have been subsequently annealed to form the perovskite phase.

The microstructure and phase evolution in films annealed at a temperature of 675 °C, which exhibit excellent ferroelectric properties and varistor-type behaviour, has been characterized by x-ray diffraction and TEM. The results indicate that there is significant diffusion of Si from the substrate into the films during the annealing process, resulting in the formation of an amorphous Si–O rich phase that wets the grain boundaries of the perovskite phase. The grains of the perovskite phase are equiaxed and consist of multiple domains. Further diffusion of Si into the film increases the fraction of the amorphous phase, which penetrates into the domain boundaries and separates the needle-like domains, thus transforming the microstructure of the film. An attempt has been made to rationalize the ferroelectric and transport properties based on the phase and microstructural evolution occurring in these films. The results of our microstructural study provide direct experimental evidence which supports the speculative explanations given by Palkar *et al* [7, 8].

Acknowledgments

The authors would like to acknowledge Professor Hamish L Fraser at the Ohio State University for providing access to the Central Electron Optics Facilities and also Suquin Meng for help with the TEM sample preparation.

References

[1] Palkar V R, Purandare S C and Pinto R 1999 *J. Phys. D: Appl. Phys.* **32** R1
[2] Polla D L and Francis L F 1996 *MRS Bull.* **21** 59
[3] Taylor G W 1977 *Ferroelectrics* **18** 17
[4] Carper M D and Phule P P 1993 *Appl. Phys. Lett.* **63** 153
[5] Selvaraj U, Prasadrao A V and Komarneni S 1994 *Mater. Lett.* **20** 71
[6] Sato E, Huang Y, Kosec M, Bell A and Setter N 1994 *Appl. Phys. Lett.* **65** 2678
[7] Palkar V R, Purandare S C, Poonawala N, Apte P R, Pinto R and Multani M S 1997 *Mater. Res. Bull.* **32** 515
[8] Palkar V R, Purandare S C, Apte P R, Pinto R and Multani M S 1997 *Appl. Phys. Lett.* **71** 3637
[9] Fujji E 1995 *Handbook of Thin Film Process Technology* ed D A Gloker and S Ismat Shah (Bristol: Institute of Physics)
[10] Lu C J, Shen H M and Wang Y N 1997 *Mater. Lett.* **34** 5
[11] 1955 *Natl Bur. Stand. Circ.* **5** 39
[12] Palkar V R, Purandare S C, Apte P R, Pinto R and Multani M S 1997 *Mater. Lett.* **32** 171
[13] Hu H and Krupanidhi S B 1994 *J. Mater. Res.* **9** 1484
[14] Moller H J 1991 *Prog. Mater. Sci.* **35** 205
[15] Pike G E and Seager C H 1979 *J. Appl. Phys.* **50** 3414